Whirlin Replacement Restores the Formation of the USH2 Protein Complex in Whirlin Knockout Photoreceptors

Junhuang Zou,[1] *Ling Luo,*[1] *Zuolian Shen,*[1] *Vince A. Chiodo,*[2] *Balamurali K. Ambati,*[1,3] *William W. Hauswirth,*[2] *and Jun Yang*[1,3]

Purpose. Whirlin is the causative gene for Usher syndrome type IID (USH2D), a condition manifested as both retinitis pigmentosa and congenital deafness. Mutations in this gene cause disruption of the USH2 protein complex composed of USH2A and VLGR1 at the periciliary membrane complex (PMC) in photoreceptors. In this study, the adeno-associated virus (AAV)-mediated whirlin replacement was evaluated as a treatment option.

Methods. Murine whirlin cDNA driven by the human rhodopsin kinase promoter (hRK) was packaged as an AAV2/5 vector and delivered into the whirlin knockout retina through subretinal injection. The efficiency, efficacy, and safety of this treatment were examined using immunofluorescent staining, confocal imaging, immunoelectron microscopy, Western blot analysis, histologic analysis, and electroretinogram.

Results. The AAV-mediated whirlin expression started at two weeks, reached its maximum level at 10 weeks, and lasted up to six months post injection. The transgenic whirlin product had a molecular size and an expression level comparable to the wild-type. It was distributed at the PMC in both rod and cone photoreceptors from the central to peripheral retina. Importantly, the transgenic whirlin restored the cellular localization and expression level of both USH2A and VLGR1 and did not cause defects in the retinal histology and function in the whirlin knockout mouse.

Conclusions. Whirlin transgene recruits USH2A and VLGR1 to the PMC and is sufficient for the formation of the USH2 protein complex in photoreceptors. The combined hRK and AAV gene delivery system could be an effective gene therapy approach to treat retinal degeneration in USH2D patients. (*Invest Ophthalmol Vis Sci.* 2011;52:2343–2351) DOI:10.1167/iovs.10-6141

From the Departments of [1]Ophthalmology and Visual Sciences, Moran Eye Center and [3]Neurobiology and Anatomy, University of Utah, Salt Lake City, Utah; and the [2]Department of Ophthalmology, University of Florida, Gainesville, Florida.

Supported by the National Institutes of Health Grants R01 EY08571 (WWH) and P30 EY014800 (core grant to the Department of Ophthalmology & Visual Sciences, University of Utah); the Hope for Vision Visionary Award (JY); the individual grant from Foundation Fighting Blindness (JY); the startup package of the Moran Eye Center, University of Utah (JY); and an unrestricted grant from Research to Prevent Blindness, Inc., New York, NY, to the Department of Ophthalmology & Visual Sciences, University of Utah.

Submitted for publication June 29, 2010; revised October 12, 2010; accepted October 28, 2010.

Disclosure: **J. Zou**, None; **L. Luo**, None; **Z. Shen**, None; **V.A. Chiodo**, None; **B.K. Ambati**, None; **W.W. Hauswirth**, AGTC Inc. (C, P); **J. Yang**, None

Corresponding author: Jun Yang, John A. Moran Eye Center, University of Utah, 65 Mario Capecchi Drive, Bldg 523, Salt Lake City, Utah 84132; jun.yang@hsc.utah.edu.

Usher syndrome manifests as retinitis pigmentosa combined with hearing loss.[1,2] It is classified into three types based on the clinical features of its hearing defects.[3–8] Usher syndrome type I (USH1) exhibits profound congenital deafness and vestibular dysfunction; USH2, the most common form, shows moderate non-progressive hearing loss without vestibular dysfunction; and USH3 has progressive hearing loss and occasional vestibular dysfunction. Currently, there is no cure for this group of diseases. Usher syndrome is a heterogeneous autosomal recessive genetic disorder. *USH2A*, *USH2C*, and *USH2D* are known to underlie USH2. They encode the proteins, usherin (USH2A), very large G protein–coupled receptor-1 (VLGR1), and whirlin, respectively.

We recently generated a whirlin knockout mouse (whirlin$^{-/-}$) with a targeted deletion at the first exon of whirlin,[9] simulating the compound heterozygosity of a Q103X mutation and a c.837+1G>A mutation discovered in USH2D patients.[10] This mouse exhibits early-onset hearing loss and progressive late retinal degeneration, resembling the symptoms in USH2 patients. In this mouse, USH2A and VLGR1 are mislocalized from the periciliary membrane complex (PMC) in photoreceptors before the onset of retinal degeneration. Additionally, the USH2A protein level is significantly reduced. Together with the findings that whirlin binds to USH2A and VLGR1 in vitro and that they colocalize in vivo,[9,11] it is believed that the three USH2 proteins form a complex at the PMC in photoreceptors and that loss of whirlin disrupts this USH2 protein complex. Further examination using electron microscopy has discovered ultrastructural abnormalities around the PMC in a small fraction of whirlin$^{-/-}$ photoreceptors before they undergo apoptosis. Retinal degeneration occurs after 28 months of age in the whirlin$^{-/-}$ mouse as shown by shortened outer segments, thinner photoreceptor nuclear layer, and reduced electroretinogram (ERG) responses.[9] Therefore, disruption of the USH2 protein complex resulting from whirlin mutations is the primary pathogenic cause underlying retinitis pigmentosa in Usher syndrome patients. Hence, restoration of this complex could be a potential and efficient therapeutic strategy for this disease.

A gene delivery system with the adeno-associated virus (AAV) and the human rhodopsin kinase promoter (hRK) has recently been developed.[12] It has been shown to successfully and specifically deliver green fluorescent protein (GFP) and aryl hydrocarbon receptor–interacting protein-like 1 (AIPL1) into both rod and cone photoreceptors in the retina.[12,13] In this study, we evaluated the kinetics and efficiency of whirlin expression mediated by this newly developed AAV-hRK system, the efficacy of whirlin replacement in restoring the USH2 protein complex in the whirlin$^{-/-}$ mouse, and the safety of the AAV-hRK-whirlin in the retina. Our study demonstrates that the AAV-hRK gene delivery system is a promising gene replacement therapeutic approach for retinal degeneration in Usher

syndrome. Our data also provide new in vivo evidence that the three USH2 proteins form a protein complex at the PMC and that whirlin is involved in the organization of this complex in photoreceptors.

METHODS

Plasmid Construction and AAV Vector Production

Whirlin cDNA was amplified from the C57BL/6 mouse retina by PCR (719–3475 bp, NM_001008791), confirmed by DNA sequencing, and inserted into the pAAV-hRK-zsGreen plasmid (kind gift of Tiansen Li, National Eye Institute). The resulting pAAV-hRK-whirlin-zsGreen and parental pAAV-hRK-zsGreen plasmids were packaged into AAV5 (Fig. 1) by the 2-plasmid cotransfection method.[14,15] Briefly, approximately 1×10^9 HEK 293 cells were cultured in Dulbecco's Modified Eagle's Medium (Hyclone Laboratories, Inc. Logan, UT), supplemented with 5% fetal bovine serum and antibiotics (cDMEM). A calcium phosphate transfection precipitation was set up by mixing a 1:1 molar ratio of AAV vector plasmid DNA and serotype specific rep–cap helper plasmid DNA. The transfection was allowed to incubate at 37°C, 7% CO_2, for 60 hours. The crude cell lysate was clarified by centrifugation and the resulting vector-containing supernatant was divided among four discontinuous iodixanol step gradients. The gradients were centrifuged at 350,000*g* for 1 hour, and 5 mL of the 60–40% step interface was removed from each gradient and combined. This iodixanol fraction was further purified and concentrated by column chromatography on a 5-ml column (HiTrap Q Sepharose; Amersham Biosciences, Piscataway, NJ) using a separation system (Pharmacia AKTA FPLC; Amersham Biosciences). The final titers for AAV-whirlin-zsGreen and AAV-zsGreen are 7.48×10^{11} and 5.32×10^{13} viral particles per millimeter, respectively, determined by real-time PCR relative to a standard.

Animals and Delivery of AAV Vectors

Whirlin and *Ush2a* knockout mice were described previously.[9,16] *Vlgr1* null mice were obtained from the BUB/BnJ mice (Jackson Laboratories, Bar Harbor, ME) by eliminating the Pde^{rd1} and $Cdh23^{ahl}$ alleles. All experiments involving animals were approved by the Institutional Animal Care and Use Committee at the University of Utah and were performed in compliance with the ARVO Statement for the Use of Animals in Ophthalmic and Vision Research.

At postnatal day 18, $whirlin^{-/-}$ mice were placed under general anesthesia with an intraperitoneal injection of avertin at the dosage of 289 mg/kg. For local anesthesia, a 0.5% proparacaine solution was applied to the cornea. Pupils were dilated with topical application of 1% tropicamide ophthalmic solution. Under a stereo microscope, a small incision was made behind the limbus with a 30.5-gauge needle. A blunt 33-gauge needle (Hamilton Company, Reno, NV) was then inserted through the incision, vitreous, and retina into the subretinal space at the posterior pole of the retina. Extra care was taken to avoid damaging the lens. One microliter of either AAV-whirlin-zsGreen or AAV-zsGreen virus at the titer of 7.48×10^{11} particles per milliliter was injected into both eyes of each mouse. Visualization of partial retinal detachment around the injection site by fundus examinations at the conclusion of injection confirmed the successful subretinal delivery.

Antibodies, Immunostaining, Immunoelectron Microscopy, and Western Blot Analysis

Polyclonal rabbit antibodies against whirlin, USH2A, VLGR1, rootletin, polyclonal chicken antibodies against blue and green opsin, polyclonal guinea pig antibody against RPGR, and monoclonal mouse antibody against rhodopsin were described previously.[9,16–18] Monoclonal mouse antibodies against dystrophin, actin, acetylated α-tubulin, and GFAP were from Sigma-Aldrich (St. Louis, MO). Alexa fluorochrome-conjugated secondary antibodies and Hoechst dye 33342 were obtained from Invitrogen (Carlsbad, CA). Horseradish peroxidase (HRP)-conjugated secondary antibodies were purchased from Jackson ImmunoResearch Laboratories, Inc. (AffiniPure; West Grove, PA).

For immunostaining of whirlin, USH2A, VLGR1, RPGR, rootletin, and acetylated α-tubulin, enucleated eyes were frozen immediately in liquid nitrogen and sectioned at 10 μm. The obtained retinal sections were fixed in 4% formaldehyde/PBS for 10 minutes (for USH2A, 2% formaldehyde/PBS for 5 minutes). For immunostaining using other antibodies, eyecups were fixed in 4% formaldehyde/PBS for 2 hours (rhodopsin) or overnight (GFAP and cone opsins), cryoprotected by incubating in 30% sucrose/PBS, and sectioned at 10 μm. The retinal sections were permeabilized by 0.2% Triton X-100/PBS for 5 minutes, blocked in 5% goat serum/PBS for 1 hour, incubated with the primary antibody in 5% goat serum/PBS at an appropriate dilution ratio at 4°C overnight, washed several times with PBS, and then incubated with the Alexa fluorochrome–conjugated secondary antibody and Hoechst dye 33342 in 5% goat serum/PBS for 1 hour. For double staining, Alexa Fluor 488 and 594 secondary antibodies were used. The stained sections were viewed and photographed on a confocal laser scanning microscope (Model FV1000, Olympus, Tokyo, Japan). The procedures for immunoelectron microscopy were exactly as described previously.[9]

For Western blot analysis, the two retinas from each mouse were dissected in PBS and homogenized in 100 μL of a radioimmunoprecipitation assay (RIPA) buffer. After centrifugation at 18,000*g* for 10 minutes, the supernatants were boiled in Laemmli buffer for 10 minutes. Then, the samples were separated by SDS-PAGE (whirlin) or a horizontal 1% agarose gel (USH2A and VLGR1, due to their extremely

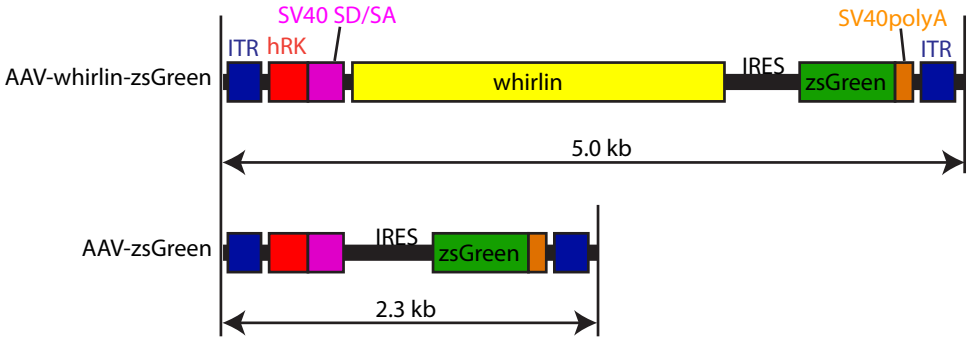

FIGURE 1. A schematic diagram of the AAV-whirlin-zsGreen and AAV-zsGreen (control) vectors. Both AAV vectors carry a zsGreen cDNA sequence. In the AAV-whirlin-zsGreen vector, whirlin and zsGreen cDNAs are separated by an internal ribosomal entry segment (IRES). Therefore, they are expected to be transcribed together and translated independently. ITR, AAV2 inverted terminal repeat; hRK, human rhodopsin kinase promoter (−112 to +183 of the proximal region)[12]; SV40 SD/SA, simian virus 40 splice donor and acceptor sites; SV40 polyA, simian virus 40 polyadenylation signal site.

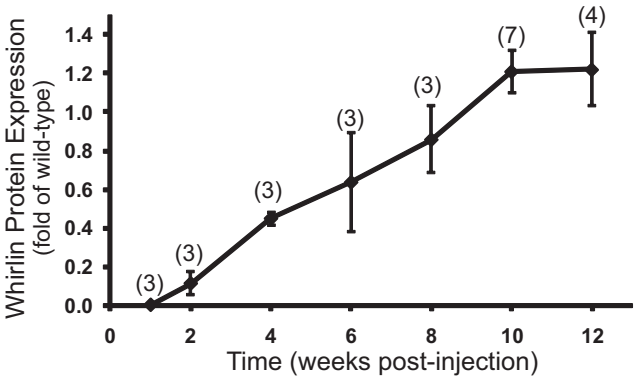

FIGURE 2. Time-dependent expression of whirlin transgene mediated by AAV5-hRK in the whirlin$^{-/-}$ retina detected by Western blot analysis. Whirlin signals were first normalized with the actin signals in their own lanes. The normalized whirlin signals in injected whirlin$^{-/-}$ retinas were then compared with the normalized endogenous whirlin signals in age-matched wild-type retinas at each time point. The number of mice measured at each time point is in the parenthesis above the line. The error bar represents the SEM.

large molecular sizes). The proteins on the gel were transferred to the PVDF membrane. The resulting PVDF membrane was sequentially subjected to blocking for 1 hour, primary antibody incubation overnight at 4°C, and secondary antibody incubation for 1 hour. Detection of the protein bands was performed using the chemiluminescent substrate and exposure to x-ray films. The intensities of protein bands were measured by densitometry and normalized using sample loading control bands. Student's *t*-tests were conducted to compare the normalized values between two different groups. A P value of <0.05 was considered to indicate a significant difference between the two groups.

Histologic and Electroretinogram Analyses

The histologic analysis was performed as described previously.[9] Briefly, measurements of photoreceptor outer segment length and outer nuclear layer thickness were made along the retinal vertical meridian at five evenly-separated locations to each side of the optic nerve head. It began at approximately 200 μm from the optic nerve head and ended at approximately 200 μm from the retinal periphery.

ERG tests were carried out using a visual diagnostic instrument (UTAS-E3000; LKC Technologies, Inc., Gaithersburg, MD). After overnight dark adaptation, mice were anesthetized with ketamine and xylazine (0.1 mg/g, 0.01 mg/g) and their pupils were dilated with 1% tropicamide. Full-field scotopic ERGs were elicited with flashes of white light in darkness. Photopic ERGs were elicited by full-field bright white flashes after 10 minutes' 35 cd/m^2 background illumination and recorded in the presence of this background illumination. Responses were monitored with an electrode placed on the cornea. A subdermal electrode was placed around the tested eye as reference electrode. A-wave amplitudes were quantified from the baseline to the peak of the cornea-negative deflection; b-wave amplitudes were quantified from the latter to the major cornea-positive peak.

RESULTS

Kinetics of Whirlin Expression Mediated by AAV5-hRK after Subretinal Injection

Murine whirlin cDNA was constructed into the pAAV-hRK-zsGreen plasmid[13] and packaged into the AAV5 vector (Fig. 1). The zsGreen cDNA, as a reporter gene, was bicistronically connected to the whirlin cDNA by an internal ribosomal entry segment. However, probably due to its low expression,[19] we could not detect zsGreen fluorescence in the injected retina using fluorescent fundus imaging. Therefore, we analyzed whirlin expression in the retina using Western blot analysis (Fig. 2). The expression of whirlin mediated by AAV5-hRK could be detected at two weeks post injection. It gradually increased and reached a plateau at 10 weeks. The expression of whirlin persisted in the retina up to six months, the longest time point we examined in this study.

Efficiency of Whirlin Expression Mediated by AAV5-hRK in the Whirlin$^{-/-}$ Retina

Western blot analysis showed that the whirlin transgene product has a molecular weight at approximately 110 kDa, identical with the endogenous whirlin in the wild-type retina (Fig. 3A). As negative controls, the whirlin$^{-/-}$ retina with and without AAV-zsGreen subretinal injection exhibited no whirlin expression. The whirlin antibody also detected some non-specific bands at approximately 50 and 24 kDa positions on the West-

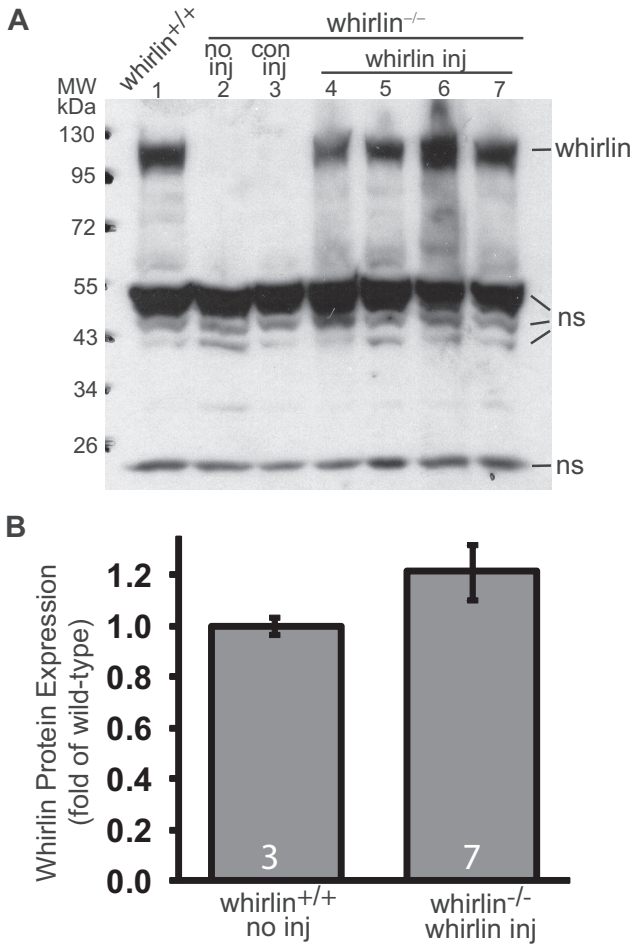

FIGURE 3. Whirlin transgene expression in the injected whirlin$^{-/-}$ retina at 10 weeks post injection detected by Western blot analysis. (**A**) A representative whirlin Western blot from one wild-type mouse (whirlin$^{+/+}$, *lane 1*) and six whirlin$^{-/-}$ mice with various treatments: no inj, no subretinal injection (*lane 2*); con inj, control subretinal injection of AAV-zsGreen (*lane 3*); whirlin inj, subretinal injection of AAV-whirlin (*lanes 4–7*, four different whirlin$^{-/-}$ mice). The whirlin band is at the position of approximately 110 kDa. Several non-specific bands (ns) at around 50 and 24 kDa are shown here as sample loading controls. (**B**) Quantification of whirlin signal intensities on the Western blot from wild-type retinas and whirlin$^{-/-}$ retinas injected with AAV-whirlin. There is no statistically significant difference between the two groups. The number of mice measured in each group is indicated at the bottom of the bars. The error bar represents the SEM.

ern blot, which served as sample loading controls to normalize whirlin signals for quantitative analysis. The expression level of whirlin transgene in the whirlin$^{-/-}$ retina was statistically the same as that in the wild-type retina (Fig. 3B). Therefore, whirlin delivered by the AAV5-hRK system expressed its full-length protein at a level comparable to the wild-type.

Immunostaining further showed that the whirlin transgene appeared as small dots between the inner and outer segment in the whirlin$^{-/-}$ retina (Fig. 4A). Faint signals in other layers of the wild-type and injected whirlin$^{-/-}$ retinas were non-specific, because they were also present in the whirlin$^{-/-}$ retina (Fig. 4A). Double staining and confocal imaging with marker proteins demonstrated that the whirlin transgene was localized above the rootlet (rootletin), below the axonemal microtubules (acetylated α-tubulin), and parallel to the connecting cilium (RPGR) (Fig. 4B). This signal pattern is similar to that in the wild-type retina, suggesting that whirlin transgene is located at the PMC in the retina. Immunoelectron microscopy further confirmed the localization of whirlin transgene at the PMC (Fig. 4C). This signal pattern of whirlin transgene was

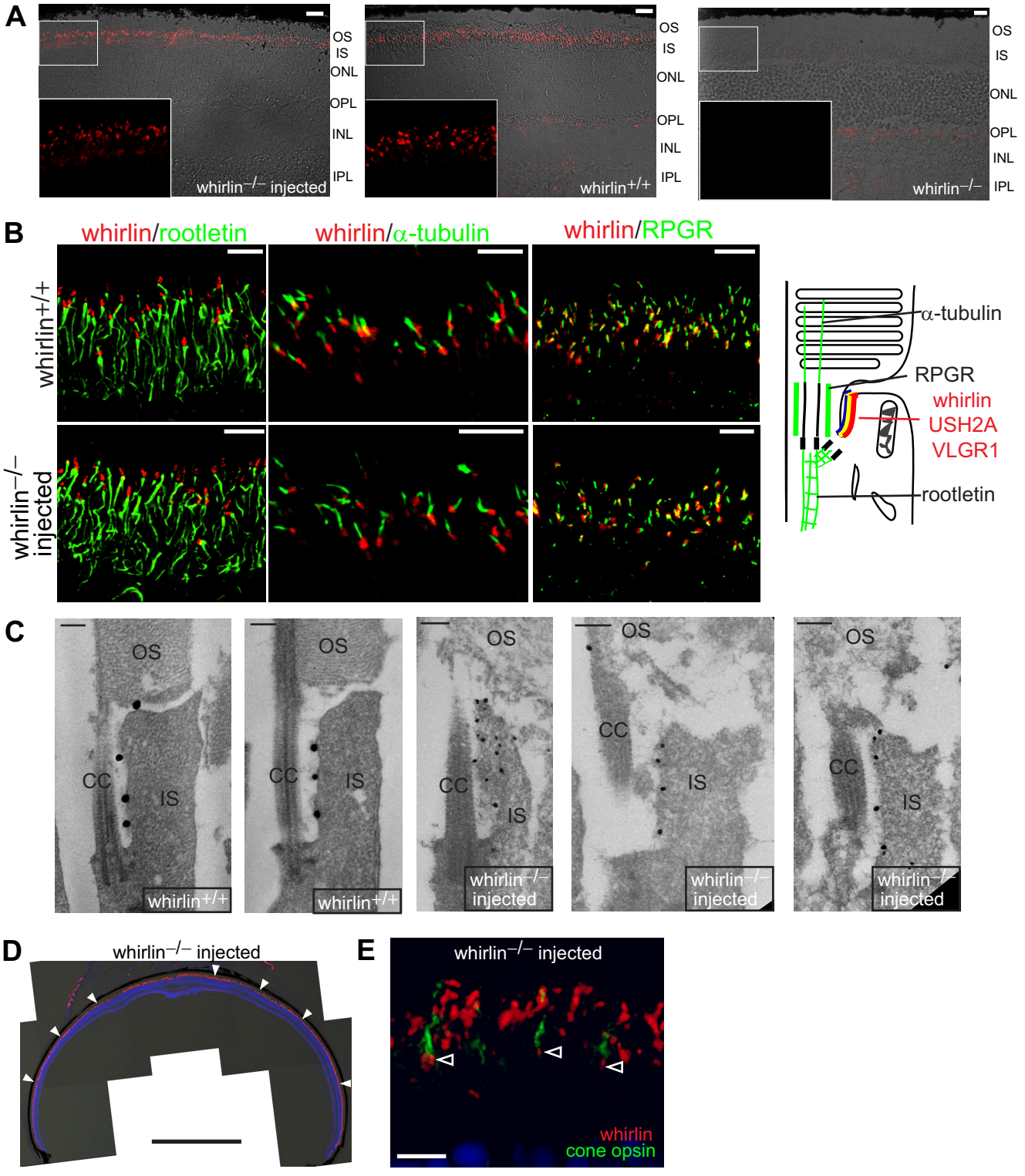

observed throughout the entire whirlin$^{-/-}$ retina (Fig. 4D). In addition, whirlin transgene was found in cone photoreceptors, as shown by double staining with mixed blue and green cone opsins (Fig. 4E). Therefore, the whirlin transgene was specifically expressed at the correct subcellular location, the PMC, in the majority, if not all, of rod and cone photoreceptors in the retina, consistent with the previous AIPL1 gene replacement study.[13]

Restoration of USH2A and VLGR1 Expression by AAV-whirlin in the Whirlin$^{-/-}$ Retina

Previously, it has been demonstrated that USH2A decreases by approximately 80% in the whirlin$^{-/-}$ retina and the residual USH2A cannot be detected at the PMC in photoreceptors by immunostaining.[9] In this study, the decrease of USH2A was consistently found in the whirlin$^{-/-}$ retina with and without injection of AAV-zsGreen (Fig. 5A). In the whirlin$^{-/-}$ retina injected with AAV-whirlin, USH2A was increased (Fig. 5A). Quantitative analysis of the USH2A signal intensity on the Western blot exhibited that the USH2A expression was increased to a level statistically close to that in the wild-type retina (Fig. 5B). In addition, immunostaining clearly demonstrated that the increased USH2A was localized between the inner and outer segment in the injected whirlin$^{-/-}$ retina (Fig. 5C). As a negative control, USH2A was not detectable in the whirlin$^{-/-}$ retina (Fig. 5C). Double staining and confocal imaging with marker proteins revealed that USH2A was enriched above the rootlet (rootletin), below the axonemal microtubules (acetylated α-tubulin), and parallel to the connecting cilium (RPGR) in the injected whirlin$^{-/-}$ retina (Fig. 5D). This signal pattern was similar to that in the wild-type retina, indicating that USH2A is localized at the PMC as it is in the wild-type retina (Figs. 5C and 5D). Therefore, whirlin transgene restores the normal expression of USH2A in whirlin$^{-/-}$ photoreceptors.

VLGR1 has been demonstrated to be undetectable at the PMC in the whirlin$^{-/-}$ retina by immunostaining in our previous study,[9] though the decrease of VLGR1 protein amount has not been determined. To evaluate the rescue effect of whirlin transgene on VLGR1 expression, we first analyzed the VLGR1 protein amount in the whirlin$^{-/-}$ retina without the AAV-whirlin injection using Western blot analysis. VLGR1 was significantly reduced in the whirlin$^{-/-}$ retina with and without subretinal injection of AAV-zsGreen (Fig. 6A). Quantitative analysis demonstrated approximately a 70% decrease in VLGR1 in the whirlin$^{-/-}$ retina (Fig. 6B). Importantly, subretinal injection of AAV-whirlin restored VLGR1 expression in the whirlin$^{-/-}$ retina to a level comparable to the wild-type retina (Figs. 6A and 6B). Further studies by immunostaining revealed that the cellular localization of VLGR1 between the outer and inner segment in photoreceptors was also restored by whirlin transgene (Fig. 6C), although some residual amount of VLGR1 was occasionally found around the nucleus in the photoreceptor (data not shown). Double fluorescent staining further demonstrated that VLGR1 was correctly positioned at the PMC by whirlin transgene in whirlin$^{-/-}$ mice (Fig. 6D).

Safety of Whirlin Replacement in the Whirlin$^{-/-}$ Retina

The whirlin$^{-/-}$ retina without any injection appears morphologically and functionally normal until the onset of retinal degeneration at 28 months of age.[9] To evaluate the safety of AAV-whirlin subretinal injection, we examined the retinal morphology and function in the whirlin$^{-/-}$ retina at six months post injection, much early before retinal degeneration started. No mislocalization of rhodopsin and cone opsins was observed in the injected photoreceptors. These proteins were exclusively distributed in the outer segment, as they were in the wild-type photoreceptor (Fig. 7A). Glial fibrillary acidic protein (GFAP) is a marker protein for retinal stress and degeneration.[18,20,21] In the injected retina, GFAP was restricted to the Müller cell endfeet and was not upregulated, similar to that in the age-matched wild-type retina (Fig. 7A). Measurement of the outer segment length and the outer nuclear layer thickness in the semithin retinal sections along the vertical meridian did not discover any changes in the injected retina (Fig. 7B). Moreover, ERG tests demonstrated that both a-wave and b-wave of injected eyes were similar to those of wild-type and whirlin$^{-/-}$ eyes (Fig. 7C). Therefore, the AAV-whirlin subretinal injection did not cause defects in the retina, as examined by staining of marker proteins, histologic analysis, and ERGs.

Discussion

This study is significant for both basic and translational research. For the basic research, we demonstrate the restoration of the integrity of the USH2 protein complex at the PMC in photoreceptors by whirlin transgene. This provides additional evidence that the three USH2 proteins form a complex in vivo and suggests that whirlin is at least one of the organizers for this complex. Therefore, our finding in this study is important for future studies on the assembly and function of the USH2 protein complex, both of which are currently largely unknown. For the translational research, we demonstrate that the combination of hRK pro-

Figure 4. Whirlin transgene expression in the whirlin$^{-/-}$ retina shown by immunostaining and immunoelectron microscopy. (**A**) Representative immunostaining images from the whirlin$^{-/-}$ retina injected with AAV-whirlin (*left panel*), the wild-type retina (whirlin$^{+/+}$, *middle panel*), and the whirlin$^{-/-}$ retina with no injection (*right panel*) at eight weeks post injection. The corresponding differential interference contrast images are superimposed with the fluorescent images. The *insets* are the enlarged view of the framed region on the original images. Scale bars, 10 μm. OS, outer segment; IS, inner segment; ONL, outer nuclear layer; OPL, outer plexiform layer; INL, inner nuclear layer; IPL, inner plexiform layer. (**B**) Representative confocal images of whirlin (*red*) double-stained with rootletin (*left, green*), acetylated α-tubulin (*middle, green*), and RPGR (*right, green*) in the wild-type retina (whirlin$^{+/+}$, *upper panels*) and the whirlin$^{-/-}$ retina injected with AAV-whirlin (*lower panels*) at six months post injection. The cartoon shows the known position of the USH2 proteins, rootletin, acetylated α-tubulin, and RPGR in wild-type photoreceptors.[9] Therefore, the localization of whirlin transgene relative to the marker proteins suggests that it is localized at the PMC in whirlin$^{-/-}$ photoreceptors. Scale bars, 5 μm. (**C**) Immunoelectron microscopy of whirlin in the injected whirlin$^{-/-}$ retina (*right three panels*) at six months post injection. The label of whirlin transgene (*black dots*) in the injected whirlin$^{-/-}$ photoreceptor is present at the PMC, similar to that in the wild-type photoreceptor (*left two panels*). CC, connecting cilium. Scale bars, 200 nm. (**D**) A low magnification view of a whirlin$^{-/-}$ retina at six months post injection of AAV-whirlin. Whirlin transgene (*red, arrowheads*) is expressed from the central to peripheral retina. Nuclear staining (*blue*) and differential interference contrast images were superimposed with the whirlin signals. Scale bar, 1 mm. (**E**) Double-staining of whirlin (*red*) and mixed blue/green cone opsins (*green*) in the whirlin$^{-/-}$ retina at 10 weeks post injection of AAV-whirlin. Whirlin transgene was localized at the PMC below the cone opsin-stained outer segment in cone photoreceptors (*arrowheads*). To view whirlin signals in cone photoreceptors, whirlin signals were enhanced in this image so that fusion of some rod photoreceptor whirlin signals is seen. Scale bar, 10 μm.

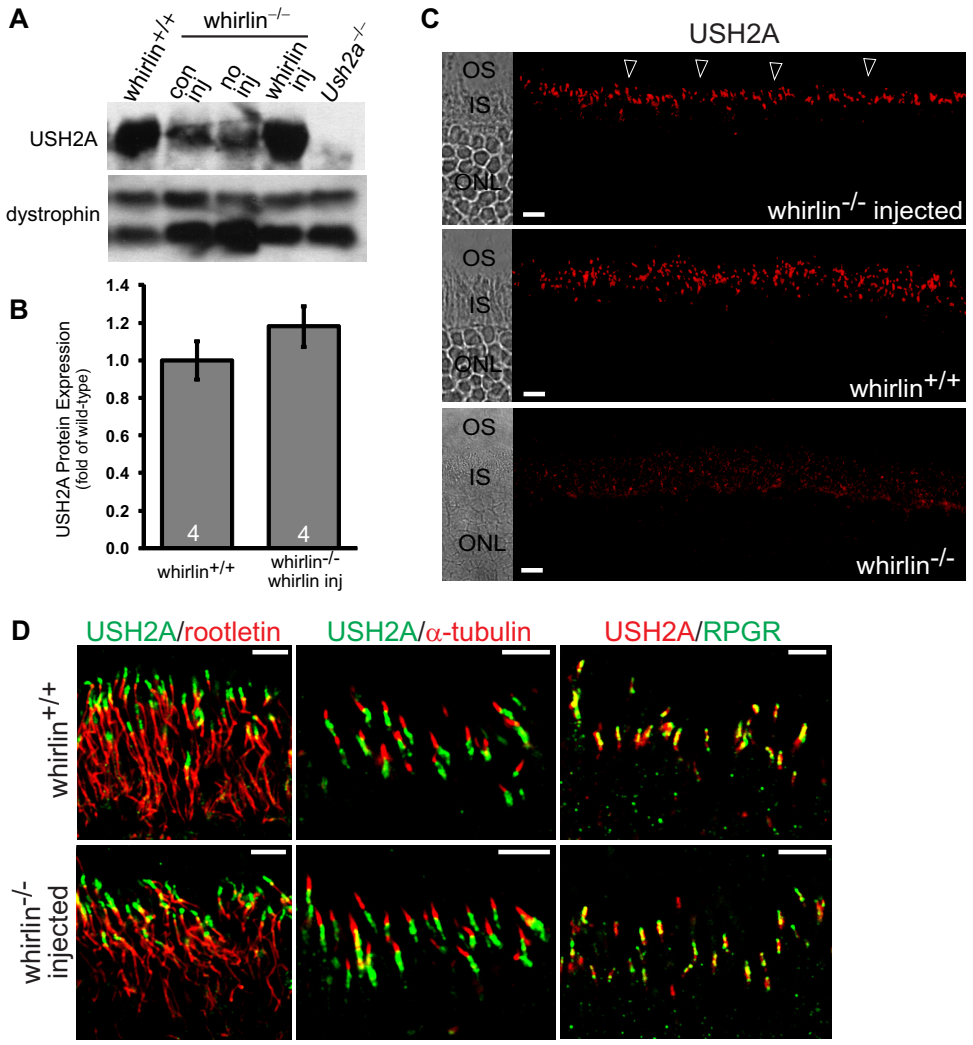

FIGURE 5. Restoration of USH2A expression in whirlin$^{-/-}$ retinas injected with AAV-whirlin. (**A**) A representative Western blot showing USH2A expression in the wild-type retina (whirlin$^{+/+}$) and the whirlin$^{-/-}$ retina with different treatments: con inj, control subretinal injection with AAV-zsGreen, 10 weeks post injection; no inj, no injection; whirlin inj, subretinal injection with AAV-whirlin, 10 weeks post injection. The *Ush2a* knockout retina (*Ush2a*$^{-/-}$) was used as a negative control. The dystrophin signal on the same blot (two bands) was used as a sample loading control. (**B**) Quantification of USH2A signal intensities on the Western blot from wild-type retinas with no subretinal injection and whirlin$^{-/-}$ retinas at 10 weeks post injection of AAV-whirlin. There is no statistically significant difference between the two groups. The number of mice measured in each group is indicated at the bottom of the bars. The error bar represents the SEM. (**C**) Immunostaining of USH2A in the whirlin$^{-/-}$ retina at 8 weeks post injection of AAV-whirlin (*top panel*, *arrowheads*), the wild-type retina (*middle panel*), and the whirlin$^{-/-}$ retina without any injection (*bottom panel*). The corresponding differential interference contrast images are shown on the *left*. OS, outer segment; IS, inner segment; ONL, outer nuclear layer. Scale bars, 10 μm. (**D**) Confocal images of USH2A double-stained with rootletin (*left*), acetylated α-tubulin (*middle*), and RPGR (*right*) in the wild-type retina (whirlin$^{+/+}$, *upper panels*) and the whirlin$^{-/-}$ retina at six months post injection of AAV-whirlin (*lower panels*). These signal patterns strongly suggest that USH2A is localized at the PMC in the whirlin$^{-/-}$ retina injected with AAV-whirlin. Scale bars, 5 μm.

moter and AAV5 targets whirlin efficiently and specifically into both rod and cone photoreceptors but not other cells in the retina. The cellular localization and expression level of whirlin mediated by this system are comparable to those of the endogenous whirlin in wild-type photoreceptors. Moreover, whirlin transgene recruits USH2A and VLGR1 to their normal cellular location at the PMC and restores their protein levels in the whirlin$^{-/-}$ retina, indicating that the whirlin transgene is fully functional and can compensate the loss of the endogenous whirlin in photoreceptors. Additionally, whirlin transgene causes no retinal morphologic and functional defects after a relatively long period post injection. These findings provide a solid basis for future studies on the AAV-mediated gene replacement therapy for retinitis pigmentosa in USH2D.

AAV has been widely used in gene therapy for retinal diseases due to its low pathogenicity and high gene-transfer efficiency. AAV5 is known to infect both photoreceptors and retinal pigment epithelium cells after subretinal delivery.[22,23] To further achieve the cellular specificity of gene targeting, the hRK promoter was recently developed.[12,13] Our study presents the whirlin transgene expression driven

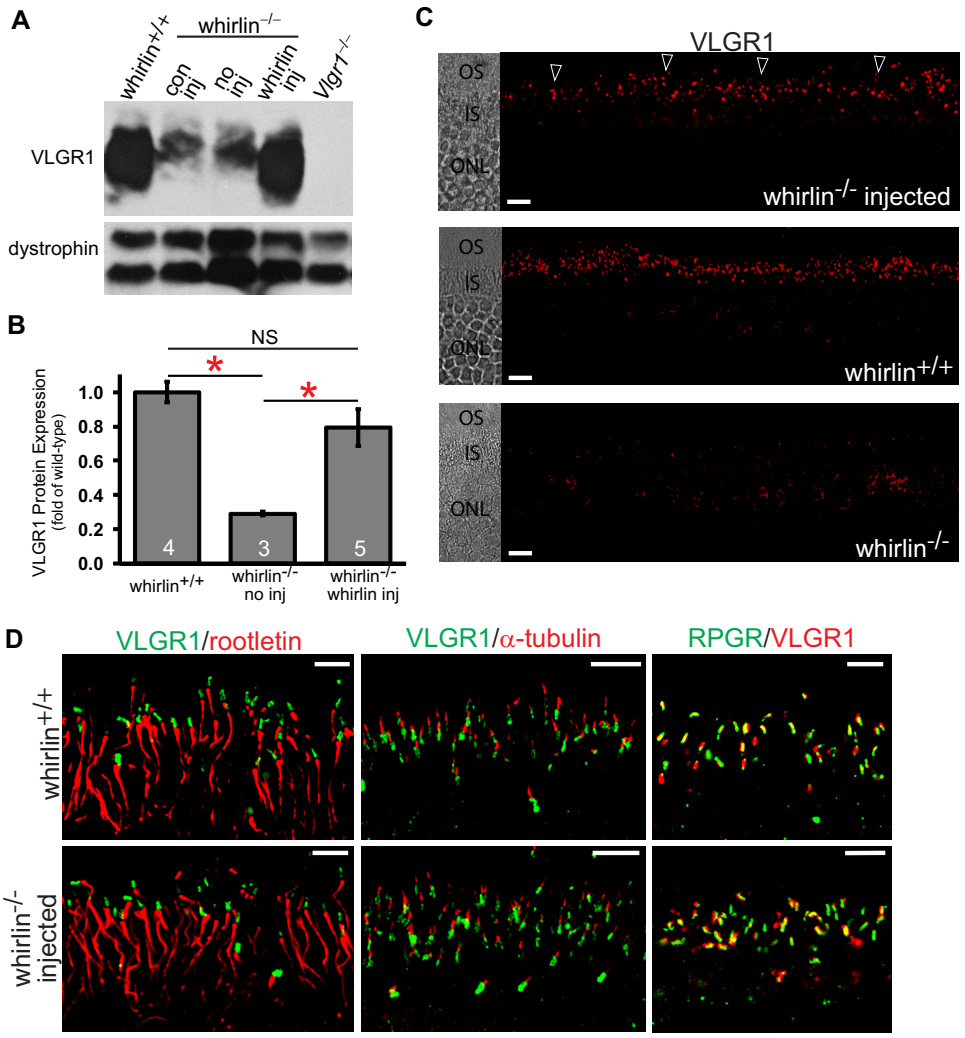

Figure 6. Restoration of VLGR1 expression in whirlin$^{-/-}$ retinas injected with AAV-whirlin. (**A**) A representative Western blot showing VLGR1 expression in the wild-type retina (whirlin$^{+/+}$) and the whirlin$^{-/-}$ retina with different treatments: con inj, control subretinal injection with AAV-zsGreen, 10 weeks post injection; no inj, no injection; whirlin inj, subretinal injection with AAV-whirlin, 10 weeks post injection. The *Vlgr1* null retina (*Vlgr1*$^{-/-}$) was used as a negative control. The dystrophin signal on the same blot (two bands) was used as a sample loading control. (**B**) Quantification of VLGR1 signal intensities on the Western blot from wild-type retinas, whirlin$^{-/-}$ retinas with no subretinal injection (no inj), and whirlin$^{-/-}$ retinas at six months post injection of AAV-whirlin (whirlin inj). The difference between wild-type retinas and whirlin$^{-/-}$ retinas and the difference between whirlin$^{-/-}$ retinas with and without the subretinal injection of AAV-whirlin are statistically significant (marked with *red asterisks*, $P < 0.05$). The difference between wild-type retinas and whirlin$^{-/-}$ retinas injected with AAV-whirlin is not statistically significant (NS). The number of mice measured in each group is indicated at the bottom of the bars. The error bar represents the SEM. (**C**) Immunostaining of VLGR1 in the whirlin$^{-/-}$ retina at eight weeks post injection of AAV-whirlin (*top panel, arrowheads*), the wild-type retina (*middle panel*), and the whirlin$^{-/-}$ retina without any injection (*bottom panel*). The corresponding differential interference contrast images are shown on the *left*. OS, outer segment; IS, inner segment; ONL, outer nuclear layer. Scale bars, 10 μm. (**D**) Confocal images of VLGR1 double-stained with rootletin (*left*), acetylated α-tubulin (*middle*), and RPGR (*right*) in the wild-type retina (whirlin$^{+/+}$, *upper panels*) and the whirlin$^{-/-}$ retina at six months post injection of AAV-whirlin (*lower panels*). These signal patterns strongly suggest that VLGR1 is correctly positioned at the PMC in the whirlin$^{-/-}$ retina injected with AAV-whirlin. Scale bars, 5 μm.

by the hRK promoter specifically in rod and cone photoreceptors throughout the retina from the center to the periphery, supporting the notion that the hRK promoter is an efficient promoter to drive the transgene expression in both cone and rod photoreceptors but not other cells in the retina. Compared to RK and AIPL1, whirlin is believed to be a low-abundance protein in photoreceptors. The close to wild-type expression level of whirlin driven by the hRK promoter shown in this study further extends the potential application of the hRK promoter to the delivery of low-abundance genes. In addition, our study first demonstrates that the onset of transgene expression in the retina mediated by the AAV5-hRK system is at two weeks post injection, which is similar to the transgene expression mediated by an AAV2/5-CMV system and detected using the in vivo imaging of the EGFP fluorescence.[23] The slow onset and long period to reach the maximum level of the transgene expression suggest that the AAV5-hRK gene transfer system may not be an appropriate gene therapy approach for early-onset forms of retinal degenerative diseases.

Our previous study demonstrates that defects in the USH2 protein complex are the main cause underlying retinal degeneration in USH2.[9] Therefore, it is critical to develop an approach to restore this complex to treat retinitis pigmentosa in USH2D patients. USH2A and VLGR1 are now the only components of the USH2 protein complex confirmed in vivo in photoreceptors. In this proof-of-principle study, we show that the whirlin transgene mediated by the AAV5-hRK system successfully correct the abnormalities of USH2A and VLGR1 expression. This restoration of the USH2 protein complex is expected to eventually delay or rescue retinal degeneration in the whirlin$^{-/-}$ mouse. Currently, the effect of AAV5-hRK-whirlin on retinal degeneration is under investigation in our laboratory. Owing to the late-onset of retinal degeneration and lack of approaches to accelerate this onset in the whirlin$^{-/-}$ mouse, completion of this evaluation will take several years.

In the past decade, gene therapy studies have been making tremendous progress in treating retinal diseases.[24–26] Results from recent clinical trials are very promising; for example, the AAV-mediated gene replacement therapy for Leber's congenital amaurosis caused by RPE65 mutations.[27–31] The AAV5-hRK gene transfer system has successfully been used to replace AIPL1 in two different *Aipl1* mutant mouse models, resembling Leber's congenital amaurosis and retinitis pigmentosa, respectively. This AIPL1 replacement corrects the retinal biochemical and functional abnormalities and eventually rescues retinal degeneration in

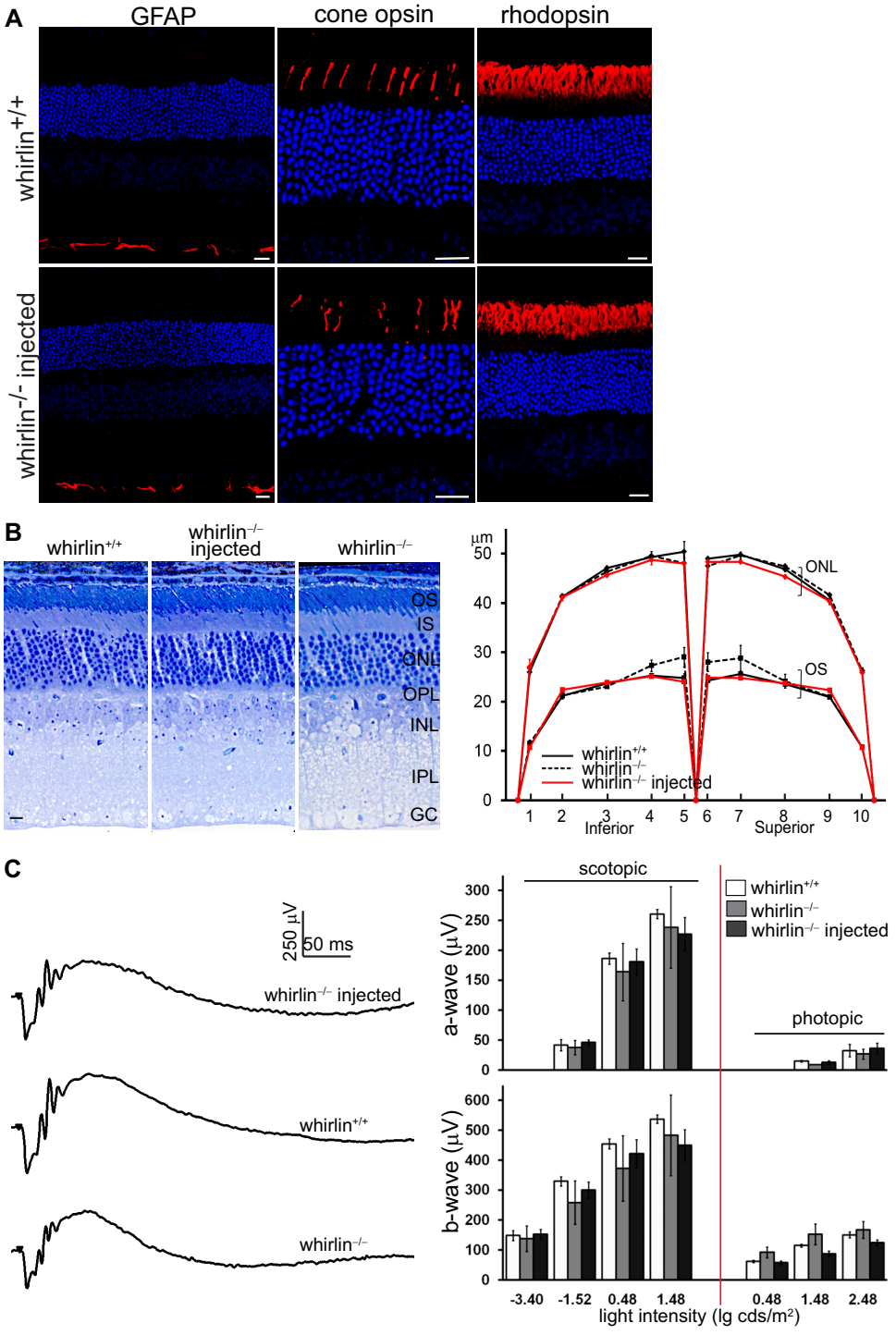

FIGURE 7. No defects found in the retinal morphology or function at 6 months post injection of AAV-whirlin. (**A**) Immunostaining of GFAP, cone opsins (mixed blue and green opsins), and rhodopsin in the wild-type retina (whirlin$^{+/+}$, *upper panels*) and the whirlin$^{-/-}$ retina injected with AAV-whirlin (*lower panels*). No mislocalization of rhodopsin and cone opsins and no changes in GFAP expression were observed in the injected whirlin$^{-/-}$ retina, compared with the age-matched wild-type retina. Scale bars, 20 μm. (**B**) Histologic analysis of the injected whirlin$^{-/-}$ retina. *Left*: representative retinal sections from whirlin$^{+/+}$, whirlin$^{-/-}$, and injected whirlin$^{-/-}$ mice. Scale bars, 10 μm. *Right*: measurement of the outer segment length (OS) and the outer nuclear layer thickness (ONL) along the retinal vertical meridian in whirlin$^{+/+}$, whirlin$^{-/-}$, and injected whirlin$^{-/-}$ mice. The number of retinas measured at each position in each group is between 3 and 6. The error bar represents the SEM. (**C**) ERG tests on the injected whirlin$^{-/-}$ eye. *Left*: representative scotopic ERG tracings from whirlin$^{+/+}$, whirlin$^{-/-}$, and injected whirlin$^{-/-}$ mice at the light intensity of 0.48 lg cds/m^2. *Right*: bar charts showing the amplitude of a-wave and b-wave of scotopic and photopic ERGs at different light intensities in whirlin$^{+/+}$, whirlin$^{-/-}$, and injected whirlin$^{-/-}$ mice. The number of eyes measured at each light intensity in each group is between 3 and 6. The error bar represents the SEM.

these models.[13] Our present study is the first to investigate the efficacy of the same gene transfer system in a mouse model for USH2, the most common form of Usher syndrome. The whirlin transgene delivered by AAV5-hRK not only normally expresses but also fully functions as a scaffold protein in photoreceptors. It corrects the key defect in the whirlin$^{-/-}$ retina. Compared to a recent publication on a lentivirus-mediated gene replacement therapy in a mouse model for USH1B,[32] our AAV5-hRK system demonstrates a much higher gene transfer efficiency into both cone and rod photoreceptors. In addition, our study shows safety of AAV-mediated whirlin replacement in the retina using various approaches. In summary, our findings are encouraging for future gene therapy studies to treat retinitis pigmentosa in USH2D patients. It may also facilitate the design of gene therapy strategies for retinitis pigmentosa in other forms of Usher syndrome, such as the ones caused by mutations in harmonin and *SANS*, which encode proteins known as scaffold proteins as well.

Acknowledgments

The authors thank Tiansen Li (National Eye Institute) for the gift of the pAAV-hRK-zsGreen plasmid, Rachael Wright (Texas A&M University)

for the RPGR antibody, Wolfgang Baehr (University of Utah) for insightful comments on the manuscript; Robert E. Marc (University of Utah), Carl Watt (University of Utah), Jiahui Yang (University of Utah), and Michael Adamian (Harvard Medical School) for immunoelectron microscopy support.

References

1. Beaty TH, Boughman JA. Problems in detecting etiological heterogeneity in genetic disease illustrated with retinitis pigmentosa. *Am J Med Genet.* 1986;24:493–504.
2. Boughman JA, Vernon M, Shaver KA. Usher syndrome: definition and estimate of prevalence from two high-risk populations. *J Chronic Dis.* 1983;36:595–603.
3. Adato A, Vreugde S, Joensuu T, et al. USH3A transcripts encode clarin-1, a four-transmembrane-domain protein with a possible role in sensory synapses. *Eur J Hum Genet.* 2002;10:339–350.
4. Geller SF, Guerin KI, Visel M, et al. CLRN1 is nonessential in the mouse retina but is required for cochlear hair cell development. *PLoS Genet.* 2009;5:e1000607.
5. Petit C. Usher syndrome: from genetics to pathogenesis. *Annu Rev Genomics Hum Genet.* 2001;2:271–297.
6. Reiners J, Nagel-Wolfrum K, Jurgens K, Marker T, Wolfrum U. Molecular basis of human Usher syndrome: deciphering the meshes of the Usher protein network provides insights into the pathomechanisms of the Usher disease. *Exp Eye Res.* 2006;83:97–119.
7. Roepman R, Wolfrum U. Protein networks and complexes in photoreceptor cilia. *Subcell Biochem.* 2007;43:209–235.
8. Williams DS. Usher syndrome: animal models, retinal function of Usher proteins, and prospects for gene therapy. *Vision Res.* 2008;48:433–441.
9. Yang J, Liu X, Zhao Y, et al. Ablation of whirlin long isoform disrupts the USH2 protein complex and causes vision and hearing loss. *PLoS Genet.* 2010;6:e1000955.
10. Ebermann I, Scholl HP, Charbel Issa P, et al. A novel gene for Usher syndrome type 2: mutations in the long isoform of whirlin are associated with retinitis pigmentosa and sensorineural hearing loss. *Hum Genet.* 2006;121:203–211.
11. van Wijk E, van der Zwaag B, Peters T, et al. The DFNB31 gene product whirlin connects to the Usher protein network in the cochlea and retina by direct association with USH2A and VLGR1. *Hum Mol Genet.* 2006;15:751–765.
12. Khani SC, Pawlyk BS, Bulgakov OV, et al. AAV-mediated expression targeting of rod and cone photoreceptors with a human rhodopsin kinase promoter. *Invest Ophthalmol Vis Sci.* 2007;48:3954–3961.
13. Sun X, Pawlyk B, Xu X, et al. Gene therapy with a promoter targeting both rods and cones rescues retinal degeneration caused by AIPL1 mutations. *Gene Ther.* 2009;17:117–131.
14. Zolotukhin S, Byrne BJ, Mason E, et al. Recombinant adeno-associated virus purification using novel methods improves infectious titer and yield. *Gene Ther.* 1999;6:973–985.
15. Hauswirth WW, Lewin AS, Zolotukhin S, Muzyczka N. Production and purification of recombinant adeno-associated virus. *Methods Enzymol.* 2000;316:743–761.
16. Liu X, Bulgakov OV, Darrow KN, et al. Usherin is required for maintenance of retinal photoreceptors and normal development of cochlear hair cells. *Proc Natl Acad Sci U S A.* 2007;104:4413–4418.
17. Yang J, Gao J, Adamian M, et al. The ciliary rootlet maintains long-term stability of sensory cilia. *Mol Cell Biol.* 2005;25:4129–4137.
18. Hong D-H, Pawlyk BS, Shang J, Sandberg MA, Berson EL, Li T. A retinitis pigmentosa GTPase regulator (RPGR)- deficient mouse model for X-linked retinitis pigmentosa (RP3). *Proc Natl Acad Sci U S A.* 2000;97:3649–3654.
19. Mizuguchi H, Xu Z, Ishii-Watabe A, Uchida E, Hayakawa T. IRES-dependent second gene expression is significantly lower than cap-dependent first gene expression in a bicistronic vector. *Mol Ther.* 2000;1:376–382.
20. Ekstrom P, Sanyal S, Narfstrom K, Chader GJ, van Veen T. Accumulation of glial fibrillary acidic protein in Muller radial glia during retinal degeneration. *Invest Ophthalmol Vis Sci.* 1988;29:1363–1371.
21. Liu X, Bulgakov OV, Wen XH, et al. AIPL1, the protein that is defective in Leber congenital amaurosis, is essential for the biosynthesis of retinal rod cGMP phosphodiesterase. *Proc Natl Acad Sci U S A.* 2004;101:13903–13908.
22. Yang GS, Schmidt M, Yan Z, et al. Virus-mediated transduction of murine retina with adeno-associated virus: effects of viral capsid and genome size. *J Virol.* 2002;76:7651–7660.
23. Auricchio A, Kobinger G, Anand V, et al. Exchange of surface proteins impacts on viral vector cellular specificity and transduction characteristics: the retina as a model. *Hum Mol Genet.* 2001;10:3075–3081.
24. Bainbridge JW, Tan MH, Ali RR. Gene therapy progress and prospects: the eye. *Gene Ther.* 2006;13:1191–1197.
25. Buch PK, Bainbridge JW, Ali RR. AAV-mediated gene therapy for retinal disorders: from mouse to man. *Gene Ther.* 2008;15:849–857.
26. Miller JW. Preliminary results of gene therapy for retinal degeneration. *N Engl J Med.* 2008;358:2282–2284.
27. Bainbridge JW, Smith AJ, Barker SS, et al. Effect of gene therapy on visual function in Leber's congenital amaurosis. *N Engl J Med.* 2008;358:2231–2239.
28. Cideciyan AV, Hauswirth WW, Aleman TS, et al. Human RPE65 gene therapy for Leber congenital amaurosis: persistence of early visual improvements and safety at 1 year. *Hum Gene Ther.* 2009;20:999–1004.
29. Hauswirth WW, Aleman TS, Kaushal S, et al. Treatment of leber congenital amaurosis due to RPE65 mutations by ocular subretinal injection of adeno-associated virus gene vector: short-term results of a phase I trial. *Hum Gene Ther.* 2008;19:979–990.
30. Maguire AM, High KA, Auricchio A, et al. Age-dependent effects of RPE65 gene therapy for Leber's congenital amaurosis: a phase 1 dose-escalation trial. *Lancet.* 2009;1597–1605.
31. Maguire AM, Simonelli F, Pierce EA, et al. Safety and efficacy of gene transfer for Leber's congenital amaurosis. *N Engl J Med.* 2008;358:2240–2248.
32. Hashimoto T, Gibbs D, Lillo C, et al. Lentiviral gene replacement therapy of retinas in a mouse model for Usher syndrome type 1B. *Gene Ther.* 2007;14:584–594.